aero-graphics
GEOSPATIAL SERVICES

LiDAR MAPPING REPORT

SALT LAKE VALLEY LIDAR AERIAL SURVEY

Submitted: June 26th, 2024

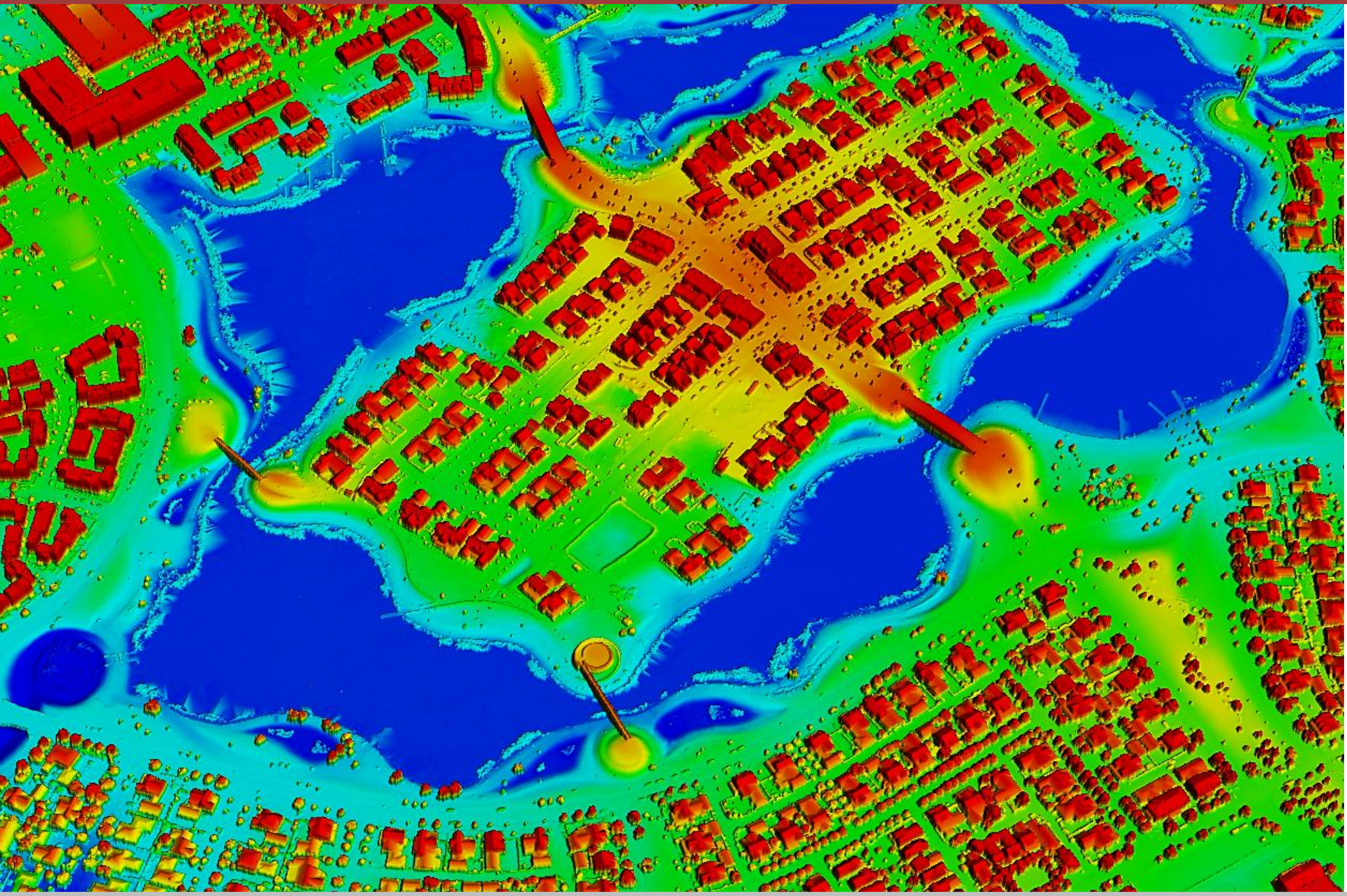

Submitted to:

Utah Department of Public Safety
Division of Emergency Management

Submitted by:

Aero-Graphics, Inc.
40 W. Oakland Avenue
Salt Lake City, UT 84115
www.aero-graphics.com

aero-graphics

LiDAR Mapping Report
Salt Lake Valley LiDAR Aerial Survey

TABLE OF CONTENTS

ATTACHMENTS

- APPENDIX C_GPS_PROCESSING_REPORT_SLV_LIDAR

1. OVERVIEW

1.1 PROJECT AREA

Aero-Graphics, Inc., a full-service geospatial firm located in Salt Lake City, Utah, was contracted by the Utah Department of Public Safety: Division of Emergency Management to acquire, process, and deliver aerial lidar data and derivative products that adhere to U.S. Geological Survey (USGS) National Geospatial Program (NGP) Lidar Base Specification 2023, Revision A, QL1 standards. The assigned project area covers approximately 487 square miles in Salt Lake County, Utah.

1.2 PROJECT DELIVERABLES

LiDAR Data	▪ **Classified point cloud LiDAR data in LAS v1.4 format**
Raster Data	▪ **DSM and DEM with a 0.5m cell size in GeoTIFF format** ▪ **MSHR at 1m cell size** ▪ **SSI at 1m cell size**
Vector Data	▪ **Breaklines in SHP format**
Report of Survey	▪ **Technical Project Report and Metadata including survey report, acquisition details, methodology, processing workflow, and results**

1.3 PROJECTION, DATUM, UNITS

Projection		**UTM Zone 12N**
EPSG		**6341**
Datum	**Vertical**	**NAVD88**
	Horizontal	**NAD83(2011)**
Units		**meters**

<u>Exhibit 1:</u> Salt Lake Valley LiDAR project boundary

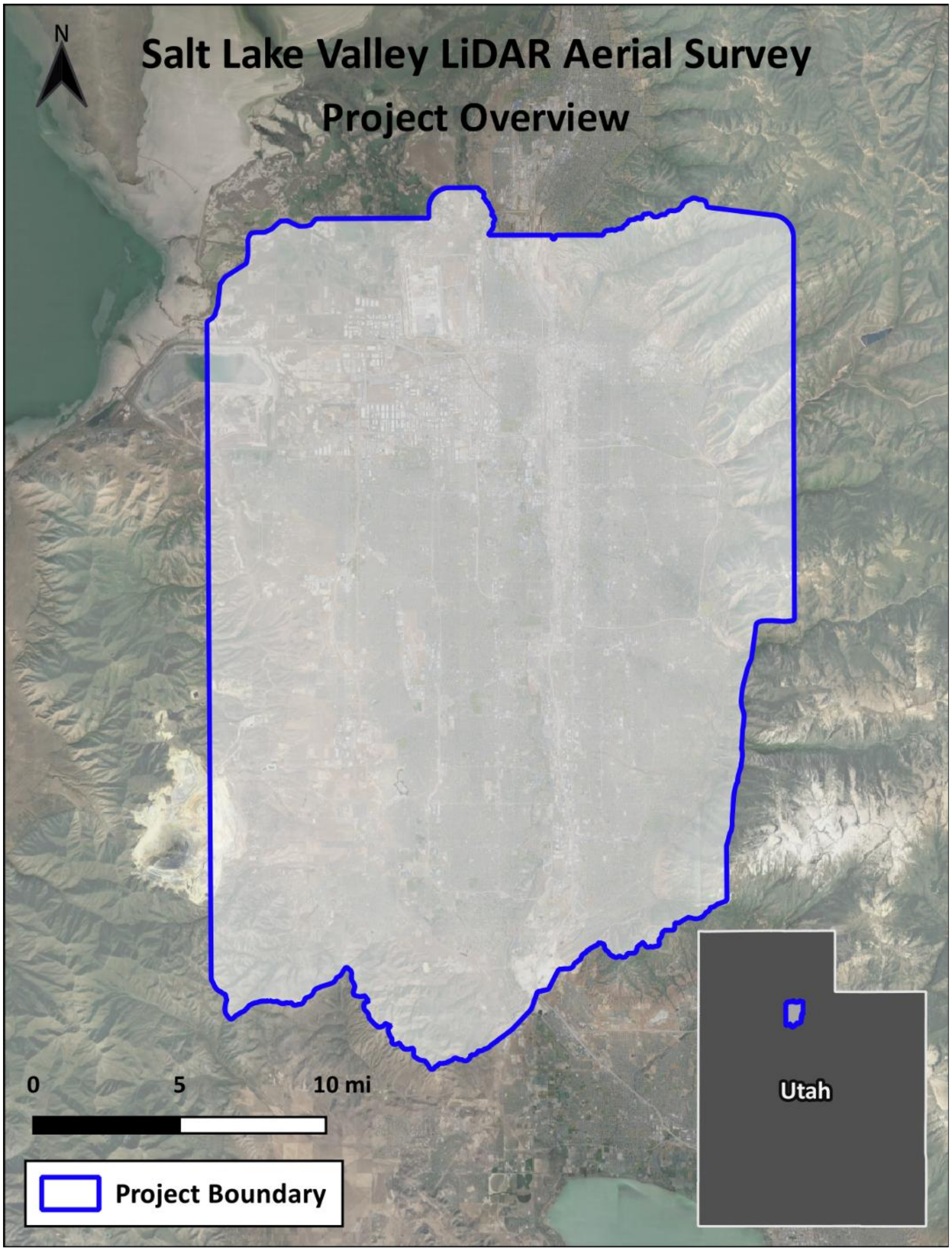

2. Acquisition

2.1 Flight Planning

Aero-Graphics Aerial Department created a unique flight plan for this project using Optech's Airborne Mission Manager (AMM) flight planning software. AMM simulates flight plans based on the project area's terrain, as well as the sensor's model, mount, and settings. These features helped ensure that all contract specifications are met in the most efficient way possible. Prior to traveling to the acquisition sites, Aero-Graphics' staff monitored all site conditions and potential weather hazards including wind, rain, snow, and blowing dust. Additionally, Aero-Graphics ensured all airspace clearances were secured by the proper officials before acquisition occurred. A summary of the flight parameters and sensor settings for the Salt Lake Valley LiDAR Aerial Survey are outlined in **Exhibit 2**.

Exhibit 2: Summary of planned flight parameters and sensor settings

Planned Specifications		
Aircraft		Cessna 310
Altitude (ft above ground level)		6,500
Speed (kts)		145
LiDAR Sensor		Optech Galaxy T2000
PRF (kHz)		1,100
Scan frequency (Hz)		115
Laser power		High (Boost)
Scan Angle	Full	28°
	From nadir	± 14°
Planned Average Point Density (p/m²)		10.39
Post Spacing at Nadir	Cross Track (m)	0.3
	Down Track (m)	0.32
Swath Width (m)		977
Sidelap (%)		20
No. of Flightlines		78

2.2 Data Acquisition

Aero-Graphics acquired LiDAR data from October 7^{th} to November 5^{th} of 2023 with a turbocharged Cessna 310 (**Exhibit 3**). The stability of this platform is ideal for efficient data collection at high and low altitudes and at a variety of airspeeds. Additionally, our Cessna 310 has been customized to house a variety of airborne sensors, and the power system and avionics have been upgraded specifically to meet aerial survey needs.

<u>Exhibit 3</u>: A Cessna 310 was the acquisition platform for this project

The Optech Galaxy T2000 was selected for this project on account of its high accuracy and efficiency (**Exhibit 4**). This sensor uses SwathTrak technology, which dynamically adjusts the scan field of view in real time to maintain a more consistent swath width over a variety of terrains. It also features up to 8 returns per pulse, which increases the vertical resolution of complex terrains. The sensor is complemented with the use of FMS Nav, which allows the system operator to monitor the point density and swath attributes of this project in real time, ensuring quality data and full coverage, as shown in **Exhibit 5**. More information about point density can be found in Section 4.4.

<u>Exhibit 4:</u> The Optech Galaxy T2000 was used for data acquisition

<u>Exhibit 5:</u> Swath data for the Salt Lake Valley LiDAR project was recorded and viewed in real-time by the sensor operator.

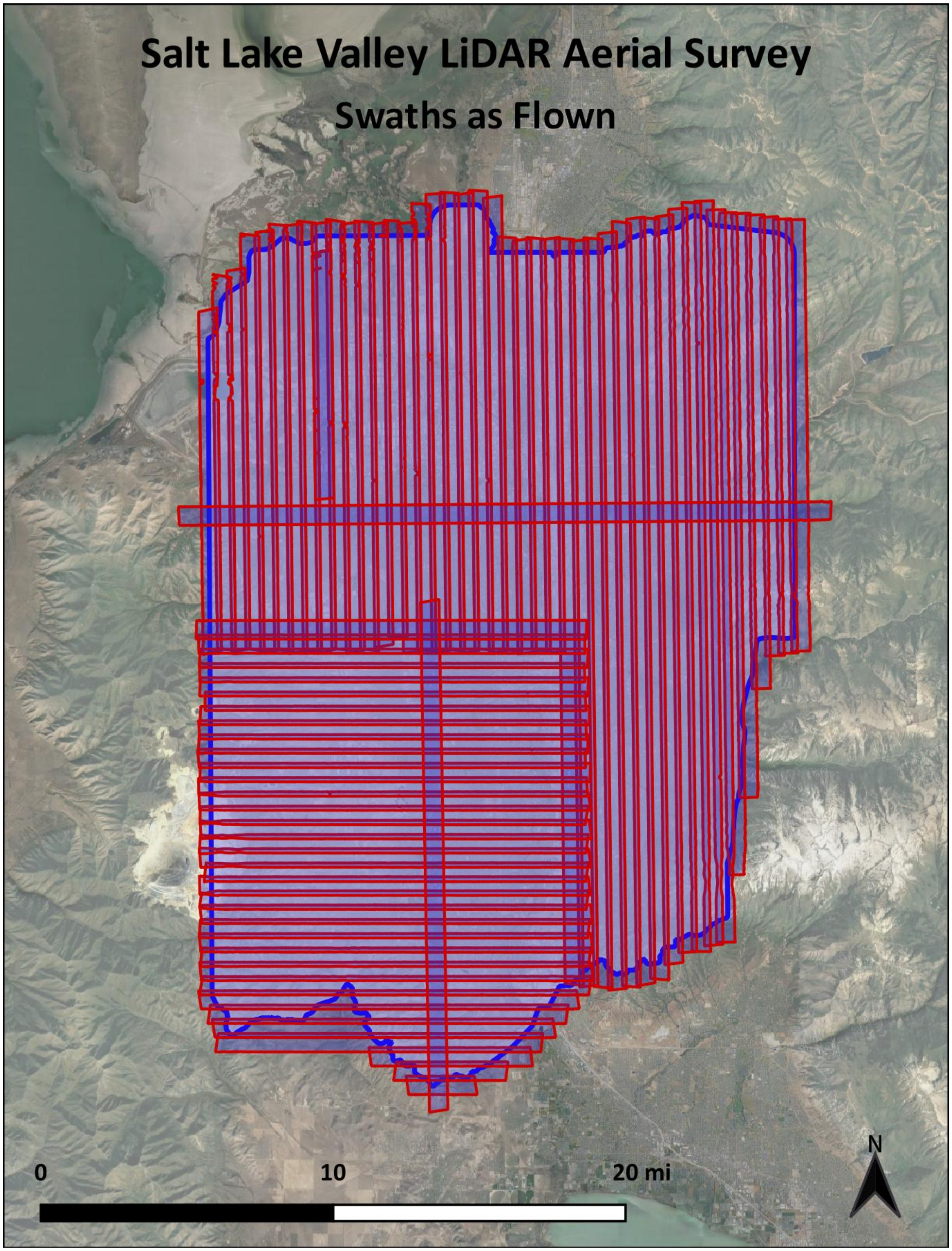

2.3 Acquisition Summary

Aero-Graphics acquired LiDAR data beginning October 7th, 2023 and concluded acquisition on November 5th, 2023.

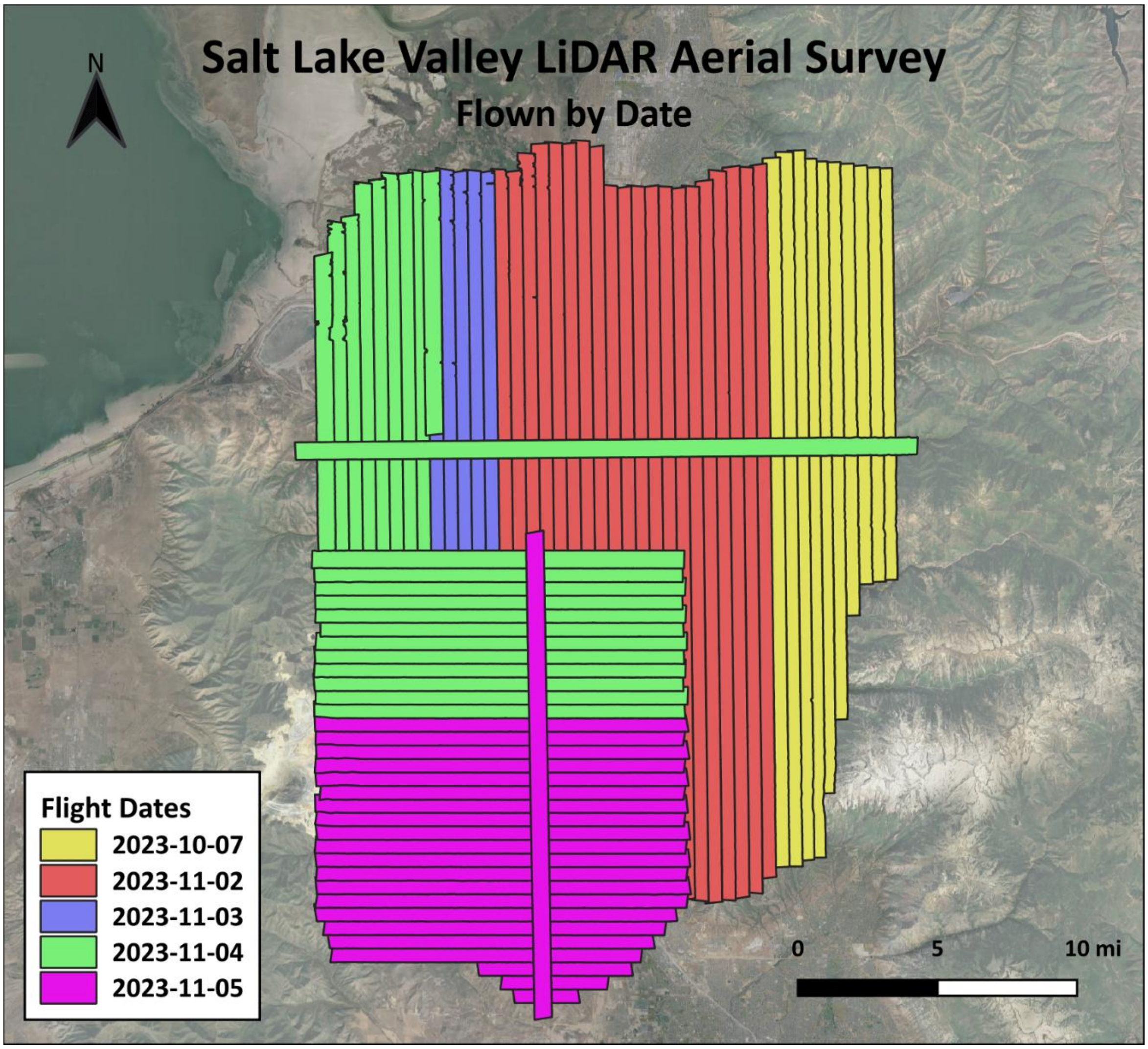

Exhibit 6: **The lines flown by date for the Salt Lake Valley LiDAR project**

The presence of ground voids should be noted in the project area. During acquisition, thick clouds of steam or smoke were observed above an industrial area. These clouds prevented the beam from hitting the ground, causing voids in the ground surface (**Exhibit 7 and 8**). The described ground voids can be found in the low_confidence_areas.shp shapefile included in the delivery.

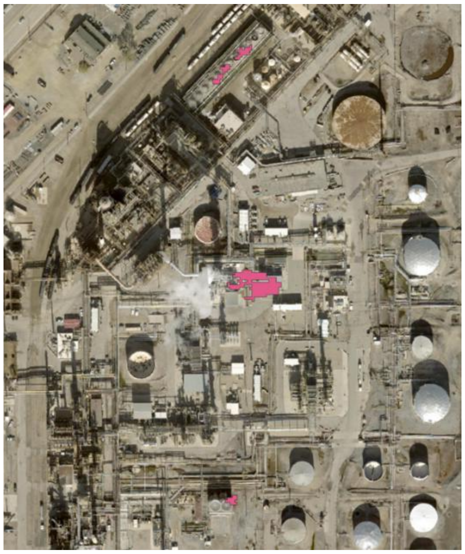

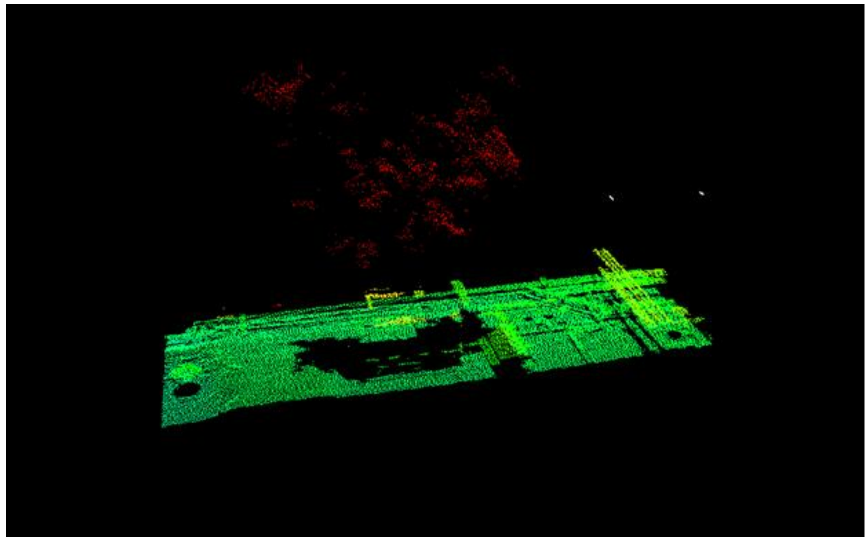

Exhibits 7 and 8: An industrial area that emanated steam or smoke, resulting in a beam obstruction and creating a void in the ground surface.

There is a location along the Jordan River which has been delineated in the low_confidence_polygons.shp where a boat ramp was being built during acquisition (**Exhibits 9 and 10**). Temporary retaining walls had been built to hold back water so the boat ramp could be built. This area appears to have erroneous "floating water" but there are valid ground returns in this location where the valid ground surface is below the water surface.

Exhibit 9. Retaining wall.

Exhibit 10. Profile of the retaining wall.

2.4 Ground Control and Check Point Survey

Aero-Graphics' professional land surveyor identified, targeted, and surveyed 20 ground control points (**Exhibit 11**) for use in data calibration as well as 65 QC check points (**Exhibit 12**) in vegetated and non-vegetated land cover classification as an independent test of accuracy for this project. A combination of precise GPS surveying methods, including static and RTK observations were used to establish the 3D position of ground control points and QC check points. Ground control coordinates can be found in Appendix A. A summary of LiDAR calibration control vertical accuracy can be found in Section 4.2 with a more detailed report in Appendix B.

Exhibit 11: Static ground control for the Salt Lake Valley LiDAR project

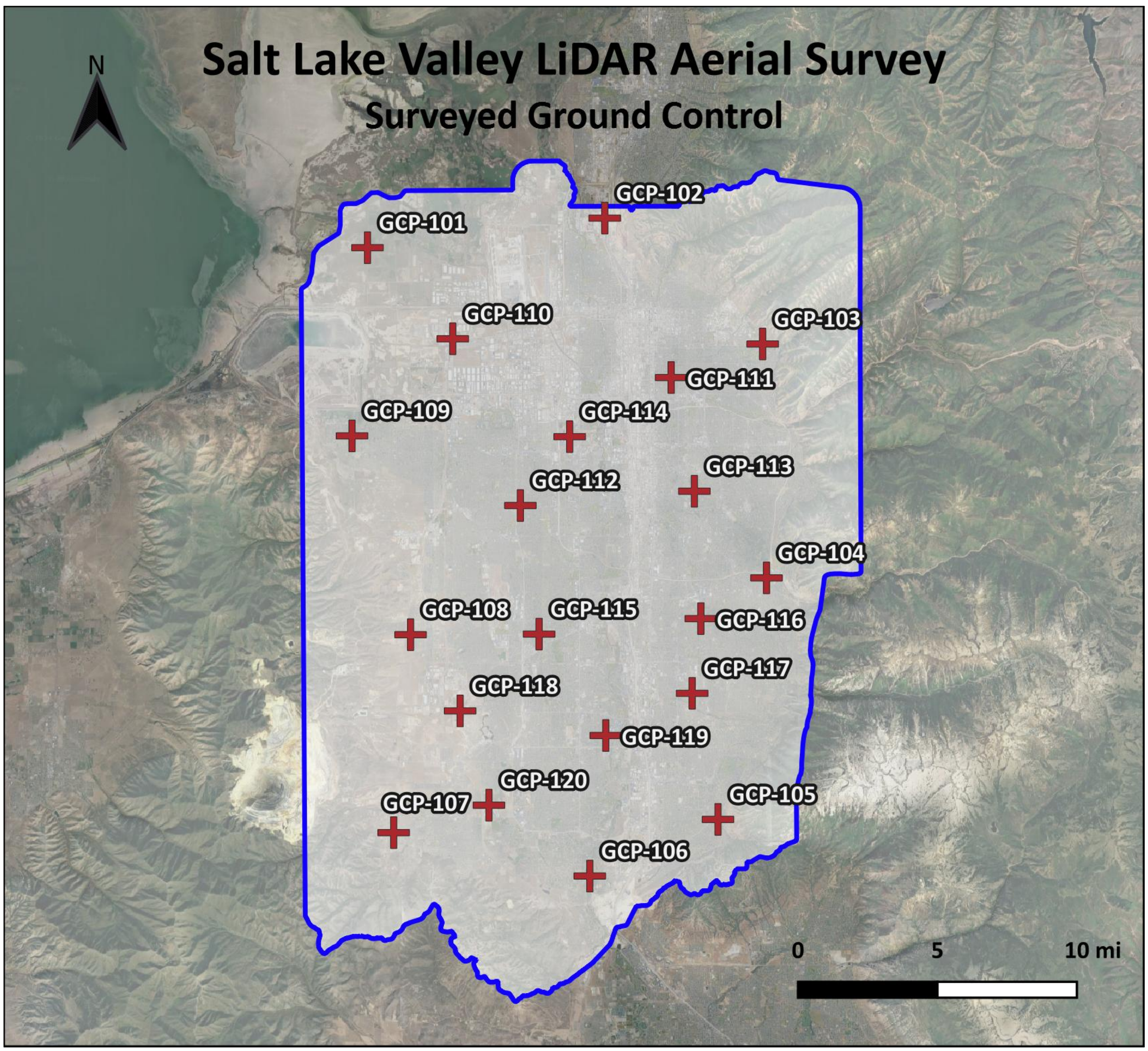

Exhibit 12: Check Points for the Salt Lake Valley LiDAR project

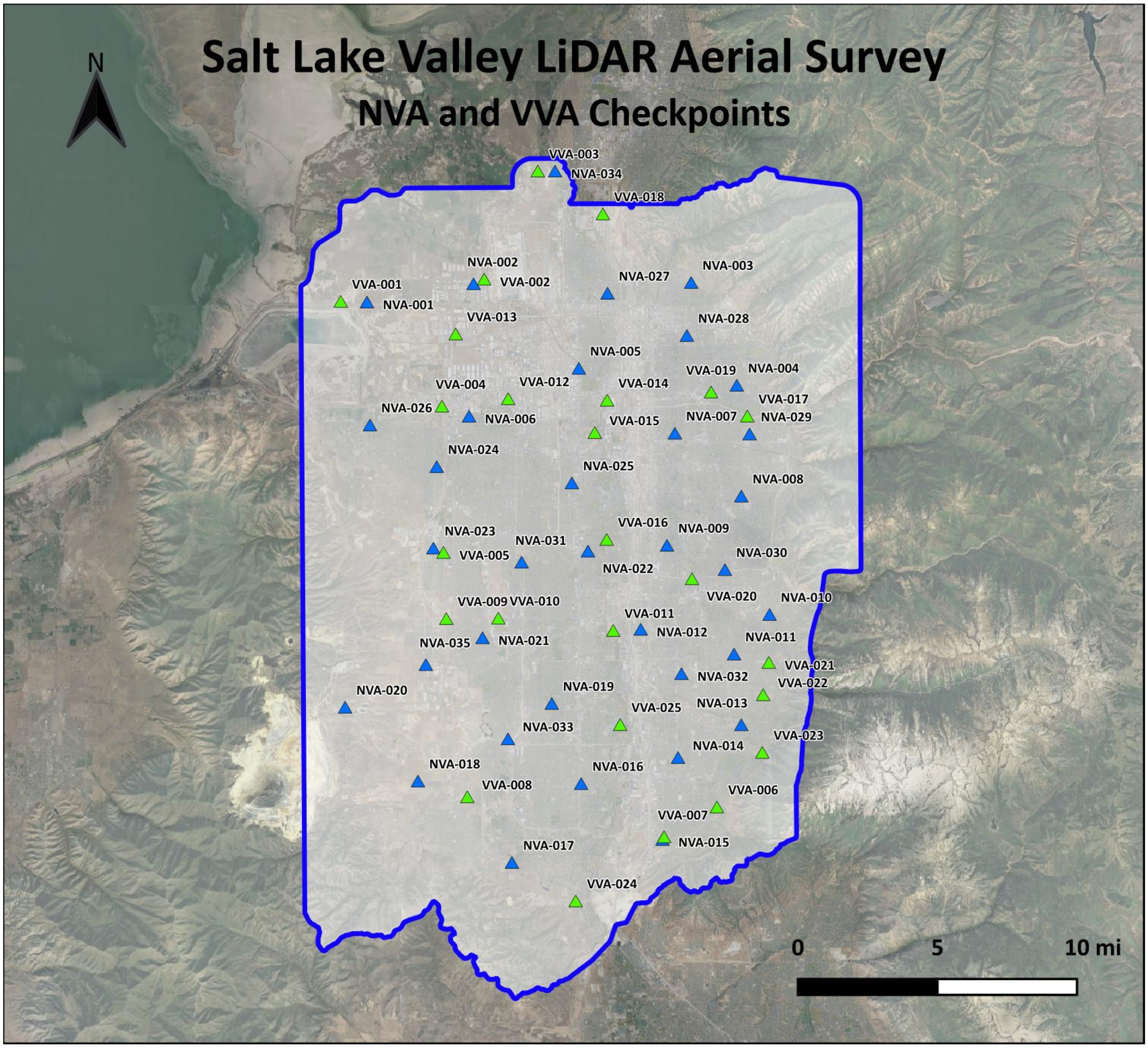

3. LiDAR Processing Workflow

1. **Absolute Sensor Calibration**. Following sensor installation, lever arm values were surveyed. A boresight mission was flown over our fully controlled local range, and when adjusted to the surveyed ground control for roll, pitch, heading, and scale errors, boresight angles were developed for application to the POS processing in subsequent steps.

2. **Kinematic Air Point Processing.** The airborne GPS positions (collected at 1-second intervals) were post-processed using Applanix's POSPac MMS GNSS Inertial software (PP-RTX). A smoothed best estimate of trajectory (SBET) was developed by combining the corrected GPS positions with 1/200-second inertial measurement unit (IMU) data, which tracked the plane's roll, pitch, and yaw throughout the flight.

3. **Raw LiDAR Point Processing (Calibration).** The SBET and LiDAR range data were combined in LMS version 4.6.2 to solve for the real-world positions of each laser point. Point cloud data was produced by flight strip in ASPRS v1.4 LAS format. Flight strips were output in the project's coordinate system. LMS also does some noise filtering which flags likely noise points as Withheld. Points flagged as Withheld by LMS are "rasterized" and inspected during acquisition QC and the noise filtering parameters are adjusted as needed on a lift-by-lift basis. These points are also reviewed during classification and can often be un-flagged if found to be valid data.

4. **Relative Calibration.** Performed relative calibration by correcting for roll, pitch, heading, and scale discrepancies between adjacent flightlines; tested resulting relative accuracy. Aero-Graphics generated swath separation images (SSI) using COTS and open-source software. These images were created from the last return of all points excluding points classified as noise and/or flagged as withheld. SSIs are made by using the Point Insertion surface method and the cell size was set to the deliverable DEM cell size. The SSIs are symbolized by the following ranges:

    I. +/- 0-8 cm: Green
    II. +/- 8-16 cm: Yellow
    III. +/- 16-24 cm: Orange
    IV. +/- 24+ cm: Red

    The output GeoTIFF rasters were tiled to the project tile grid, clipped to the master DPA, and formatted (including defining the CRS which matches the project CRS) using GDAL software, version 2.4.0. These results are presented in Section 4.1.

    a. A **Dz Ortho Raster** was generated as part of this process (**Exhibit 13)**. This raster identifies clusters of large residuals and differences in measured elevations between overlapping flightlines. These errors are usually caused by topographic relief or environmental factors and require manual adjustments to correct. In most cases, multiple iterations of the Dz ortho raster are created to aid in fine tuning relative calibration parameters.

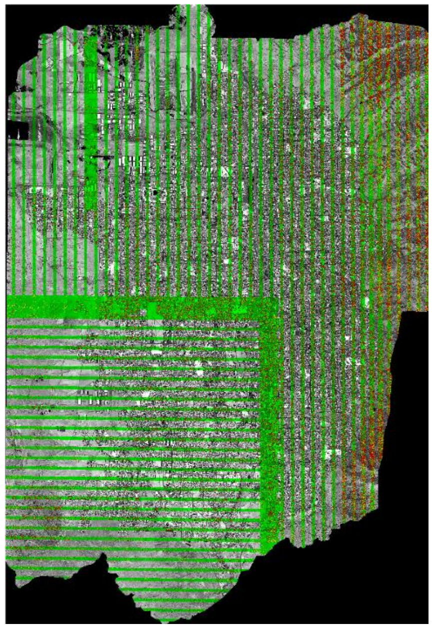

Exhibit 13: A Dz ortho raster generated for the Salt Lake Valley LiDAR project

5. **Calibration QC.** Calibrated data is reviewed to ensure the project meets specifications. File formatting is checked for consistency. The calibrated data is reviewed against control to confirm it meets the required Vertical Accuracy Class (Results are presented in Section 4.2). Point density is analyzed and questionable areas of overlap are investigated and measured in LP360.

6. **Long/Short Filtering & Tiling.** After calibrated swaths are reviewed, additional noise filtering is applied if needed and the LAS swaths are tiled to the project tiling scheme using TerraScan functionality. Extremely long and short returns were also filtered out as outliers and classified to a temporary class to be reclassified to low or high noise after completion of ground point classification.

7. **Classified LAS Processing.** The point classification was performed with the ASPRS classes described in **Exhibit 14.** The bare-earth surface is classified using a combination of TerraScan macro functionality as well as proprietary software. The bare-earth surface is then manually reviewed and corrected to ensure correct classification on the Class 2 (Ground) points. Quality Control (QC) DEMs are then created using Whitebox Tools Tin Gridding software and automated and manual means are used to generate QC calls. The QC Dems are also symbolized as hillshades in QGIS and a manual qualitative review is conducted by an Aero-

Graphics technician to identify any remaining artifacts. Each resulting QC call is then addressed using functionality provided by TerraScan.

Exhibit 14: The ASPRS classes used in lidar point classification

ASPRS Version 1.4 minimum point cloud classification scheme		
CLASS #	**CLASS NAME**	**DESCRIPTION**
1	Processed, but unclassified	Points that do not fit any other classes
2	Bare earth	Bare earth surface
7	Low noise	Low points identified below surface
9	Water	Points inside of lakes/ponds
17	Bridge decks	Points on bridge decks
18	High noise	High points identified above surface
20	Ignored ground	Points near breakline features; ignored in DEM creation process

8. **Breakline Collection**. Ground LiDAR points were used to create a bare earth surface model, which was used to heads-up digitize 2D breaklines of inland streams and rivers with a 30 m nominal width, and inland ponds and lakes of 2 acres or greater surface area. Elevation values were assigned to all inland ponds and lakes, inland pond and lake islands, and inland stream and river islands, using LP360 functionality. Elevation values were assigned to all inland streams and rivers using Aero-Graphics, Inc.'s proprietary software. All ground LiDAR data inside of the collected inland breaklines were then classified to water using TerraScan macro functionality. All points that fall within a 2 x Nominal Point Spacing buffer from each breakline are reclassified to Class 20 (ignored ground).

   The breakline files were translated to ESRI shapefile format and were reviewed against LiDAR intensity imagery to verify completeness of capture. All breaklines were compared to triangular irregular networks (TINs) created from ground-only points prior to water classification. To ensure the breaklines matched the LiDAR within accepted tolerances, the horizontal placement of breaklines was compared to terrain features, and the breakline elevations were compared to LiDAR elevations. Some deviation is expected between breakline and LiDAR elevations due to monotonicity enforcement, connectivity, and flattening rules that are enforced on the breaklines. Once horizontal placement and vertical variance was reviewed, all breaklines were checked for topological consistency and data integrity using a combination of ESRI ArcMap tools and proprietary tools.

   Breaklines were collected at bridges but not culverts. The distinction between bridges and culverts was based on the following guidelines: Bridges are structures carrying a road, path, railroad, canal, aircraft taxiway, or any other transit between two locations of higher elevation over an area of lower elevation. A bridge may traverse a river, ravine, road, railroad, or other obstacle. "Bridge" also includes but is not limited to aqueduct, drawbridge, flyover, footbridge, overpass, span, trestle, and viaduct. In mapping, the term “bridge” is distinguished from a roadway over a culvert in that a bridge is an elevated deck that is not underlain with earth or soil. Culverts are a tunnel carrying a stream or open drainage under a road or railroad or through another type of obstruction to natural drainage.

Waterbody breaklines in marshy areas were mainly collected to delineate open water, but revisions have been made in many areas where there was an elevation decrease immediately adjacent to the waterbody breakline.

9. **Hydro-Flattened Raster DEM Creation.** A hydro-flattened raster digital elevation model (DEM) was created from a TIN surface generated using ground classified LiDAR points. The hydro-flattened DEMs, clipped to the project tile grid, were generated in LP360 using the hydro and DTM breaklines collected. The tiled DEMs were reviewed at a scale of 1:5,000 to look for artifacts caused by the DEM generation process and to verify correct and complete hydro-flattening was applied. Upon correction of any outstanding issues, the DEM data was loaded into QGIS for its second review and to verify corrections. Final DEMs are formatted using GDAL software version 2.4.0.

10. **DSM/First Return Raster Creation.** A first-return raster digital surface model (DSM) was created using the first-return LiDAR points, which was then tiled in the GeoTIFF format using LP360 and automated scripting routines. Each surface was reviewed in QGIS to check for any surface anomalies or incorrect elevations found within the surface.

11. **Maximum Surface Height Rasters Creation**. MSHRs are delivered as tiled GeoTIFFs (32-bit, floating point), with the tile size and naming convention matching the project tile grid. All points, excluding points flagged as withheld, are used to produce MSHRs using PDAL software. The rasters are produced with a binning method in which the highest elevation of all lidar points intersecting each pixel is applied as the pixel elevation in the resulting raster. Final MSHRs are formatted using GDAL software version 2.4.0, spatially defined to match the project CRS, and the cell size equals 2x the deliverable DEM cell size.

12. **LAS and GeoTIFF Formatting.** LAS files are formatted using PDAL software. Any extra dimensions generated during classification are removed and the projection wkt string is written to the header. Tif files are compressed using LZW compression, and headers are formatted using a combination of GDAL and proprietary software. The DEMs and DSMs are then processed through COTS software to produce the COG formatted deliverable elevation data.

4. Accuracy Testing and Results

4.1 Relative Calibration Accuracy Results

Inter-swath relative accuracy is defined as the elevation difference in the overlapping area of parallel swaths. The elevation difference between these overlapping areas is used to measure the between-swath relative accuracy of the dataset. During calibration, this process is carried out to verify consistency from swath to swath, but as a quality assurance measure it can also point toward the internal consistency of the overall dataset. This testing was performed using COTS which produces an overall DZ ortho, summary statistics for each swath pair, and global statistics. Each of the QC products is inspected by an Aero-Graphics calibration technician who determines if further corrections need to be applied.

The inspection consists of the following steps:

1. The calibration DZ produced by the COTS Lidar calibration software is brough into a GIS and overlayed on satellite imagery. The technician looks for any anomalies and pays close attention to roads as well as roofs and other sloped areas which can indicate issues with the vertical and horizontal alignment. The technician also monitors swath edges closely which may indicate that the Lidar sensor's calibration profile may need a slight adjustment.
    a. The DZ produced during calibration uses a continuous color ramp based on the range of the resulting DZ values.

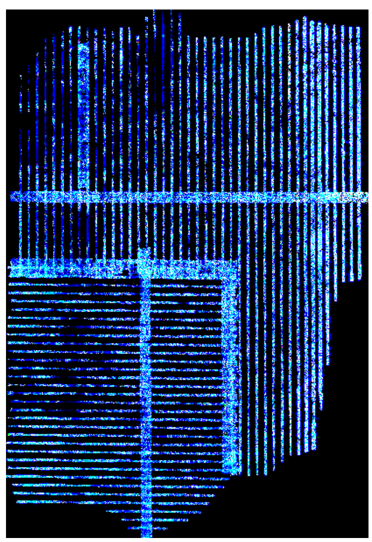

Exhibit 15: Example of calibration DZ

b. Color ramp of calibration DZs: 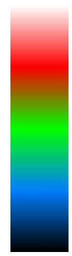

2. The calibration technician then inspects the pair wise statistics to see if any swath pairs are misaligned. Testing for this project was based on a total of 282 pairs covering a total of 475 square kilometers. For this project all pairs displayed similar RMS DZ results and were found to be well below acceptable levels.

3. Lastly the calibration technician inspects the global statistics to determine if the overall inter-swath accuracy of the project is within project specifications. A qualitative review of the deliverable swath separation rasters is also done as soon as calibration is complete, and the Lidar data has been tiled for further processing. This is done to validate the swath separation rasters as well as identify any potential issues the calibration technician may have missed. This process is described in section 3.4 of this report.

Salt Lake Valley LiDAR Aerial Survey project area: (282 pairs, 475 square kilometers)

- Inter-swath relative accuracy **average** of 0.007 m

Intra-swath Precision is a measure of the expected precision of the laser ranging measurement. The metric is derived by calculating the variation in elevation values across a smooth flat surface and was calculated using a kernel size of 1.2 m around each control point. A total of 21 swaths were tested. The intra-swath precision average was found to be 0.020 m. The minimum, maximum, and standard deviation of the intra-swath *accuracy* was found to be -0.05 m, 0.03 m, and 0.023 m respectively. This was performed in Bayes Strip Align which produces a detailed report of many calibration quality assurance metrics.

4.2 Calibration Control Vertical Accuracy

Vertical absolute accuracy reports were generated as a quality assurance check. The location of each control point is displayed in the Surveyed Ground Control map in **Exhibit 11**. Detailed results for each point are included in **Appendix B**.

Exhibit 16: Calibration control vertical accuracy results summary

Calibration Control Accuracy$_z$: Salt Lake Valley LiDAR Project Area	
Average Error = -0.030 m	Average Magnitude = 0.040 m
Minimum Error = -0.090 m	RMSE = 0.043 m
Maximum Error = +0.020 m	σ = 0.030 m
Survey Sample Size: n = 20	

4.3 Point Cloud Testing

The project specifications require that Non-Vegetated Vertical Accuracy (NVA) and Vegetated Vertical Accuracy (VVA) be computed for raw LiDAR point cloud swath files. NVA is defined as the elevation difference between the LiDAR ground surface and statically surveyed ground control points collected in open terrain (bare soil, sand, rocks, and short grass) as well as urban terrain (asphalt and concrete surfaces). The NVA for this project was tested with 35 check points. The VVA for this project was tested with 30 check points. These check points were not used in the calibration or post-processing of the LiDAR point cloud data. Elevations from the unclassified LiDAR surface were measured for the xy location of each check point. Elevations interpolated from the LiDAR surface were then compared to the elevation values of the surveyed control points.

The bare-earth LiDAR dataset was designed to meet or exceed ASPRS Positional Accuracy Standards at the 10 cm vertical accuracy class. Absolute accuracy for non-vegetated areas (NVA) must be accurate within 10.0 cm (0.32 ft) RMSEz and 19.6 cm (0.64 ft) at the 95% confidence level. The tested NVA for this dataset was found to be accurate within 5.1 cm (0.17 ft) in terms of the RMSEz. The resulting NVA stated at the 95% confidence level (RMSEz x 1.96) is 11.5 cm (0.37 ft). Therefore, this dataset meets the required NVA of 19.6 cm (0.64 ft) at the 95% confidence level as defined by the National Standards for Spatial Data Accuracy (NSSDA).

The tested Vegetated Vertical Accuracy (VVA) of the point cloud dataset was found to be 4.8 cm (0.16 ft). The resulting NVA stated at the 95% confidence level (RMSEz x 1.96) is 9.5 cm (0.31 ft). Therefore, this dataset meets the required VVA of 30.0 cm based on the 95th percentile error.

4.4 Digital Elevation Model Testing

The project specifications require the accuracy of the derived DEM be calculated and reported in two ways: (1) Non-Vegetated Vertical Accuracy (NVA) calculated at a 95% confidence level in "bare earth" and "urban" land cover classes and (2) Vegetated Vertical Accuracy (VVA) in all vegetated land cover classes combined calculated based on the 95th percentile error. The NVA for this project was tested with 35 check points. The VVA was tested with 30 check points.

The Non-Vegetated Vertical Accuracy (NVA) for this dataset was tested by sampling the DEM elevation value at each NVA checkpoint and differencing the sampled DEM Value and the statically surveyed NVA checkpoint elevation value. The resulting RMSEz of the DEM values were found to be 6.0 cm (0.20 ft). The resulting accuracy stated as the 95% confidence level (RMSEz x 1.96) is 11.7 cm (0.38 ft). Therefore, this dataset meets the required NVA of 19.6 cm at the 95% confidence level.

The tested Vegetated Vertical Accuracy (VVA) for this dataset captured from the DEM using bi-linear interpolation for all classes was found to be 5.1 cm (0.17 ft). Therefore, this dataset meets the required VVA of 30 cm based on the 95th percentile error.

4.6 Data Density

The goal for this project was to achieve a minimum LiDAR point density of **8.0** points per square meter. First return density is the best representation of the quality of the acquisition because the density of first returns is independent of vegetation and other random factors that could increase the overall point density. The acquisition mission achieved an actual average of **18.2** points per square meter for the first returns. Please note that ground water and other random factors could decrease the overall point density.

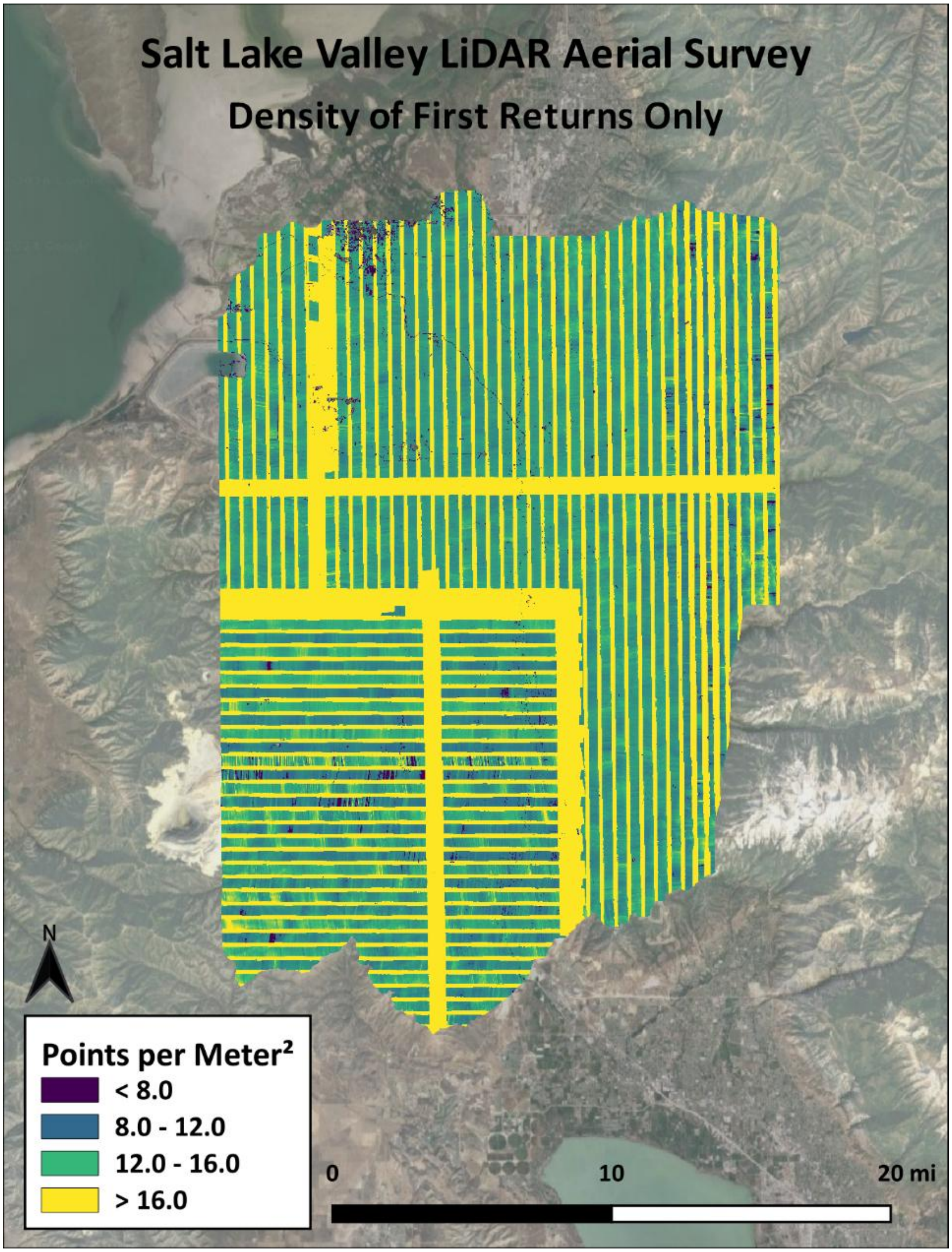

Exhibit 17: Density of first returns only in points per meter² for the Salt Lake Valley LiDAR project.

Appendix A – Check Points

Survey Point	Salt Lake Valley LiDAR Aerial Survey		
	Easting	Northing	Elevation (m)
NVA-001	408621.96	4513938.17	1286.96
NVA-002	414741.14	4514909.39	1287.83
NVA-003	427211.66	4514848.50	1477.32
NVA-004	429768.89	4508955.87	1387.42
NVA-005	420720.14	4510013.07	1290.39
NVA-006	414394.76	4507349.00	1297.07
NVA-007	426189.52	4506247.07	1301.53
NVA-008	429969.98	4502618.32	1358.70
NVA-009	425673.79	4499845.66	1321.83
NVA-010	431528.38	4495830.80	1500.51
NVA-011	429465.89	4493585.10	1468.41
NVA-012	424117.29	4495052.90	1334.74
NVA-013	429842.99	4489530.75	1501.79
NVA-014	426187.91	4487688.17	1367.88
NVA-015	425246.90	4483000.33	1375.23
NVA-016	420601.06	4486255.40	1351.21
NVA-017	416568.90	4481777.99	1461.39
NVA-018	411215.23	4486504.48	1528.48
NVA-019	418960.38	4490860.04	1388.24
NVA-020	407077.33	4490783.69	1668.41
NVA-021	415025.06	4494669.50	1431.01
NVA-022	421133.24	4499560.49	1317.10
NVA-023	412259.72	4499828.76	1498.79
NVA-024	412505.34	4504489.05	1350.13
NVA-025	420251.56	4503466.66	1304.41
NVA-026	408707.19	4506914.09	1300.73
NVA-027	422413.88	4514282.10	1286.96
NVA-028	426934.90	4511824.90	1313.25
NVA-029	430476.48	4506161.33	1404.63
NVA-030	428987.78	4498419.20	1353.52
NVA-031	417319.79	4498970.80	1383.72
NVA-032	426434.79	4492488.57	1382.95
NVA-033	416421.30	4488863.84	1430.40
NVA-034	419482.59	4521286.86	1286.12
NVA-035	411750.61	4493169.90	1518.23
VVA-001	407116.98	4513994.19	1284.92
VVA-002	415352.44	4515165.50	1286.46
VVA-003	418493.67	4521296.82	1285.31

VVA-004	412844.82	4507941.25	1293.36
VVA-005	412838.61	4499574.45	1485.19
VVA-006	428397.14	4484834.42	1398.29
VVA-007	425341.14	4483154.50	1372.75
VVA-008	414041.79	4485567.20	1473.41
VVA-009	412956.67	4495787.86	1479.43
VVA-010	415948.41	4495777.97	1405.77
VVA-011	422537.29	4495001.27	1324.04
VVA-012	416648.12	4508318.09	1294.86
VVA-013	413680.27	4512050.83	1290.79
VVA-014	422325.16	4508170.93	1291.80
VVA-015	421598.18	4506331.92	1293.32
VVA-016	422215.52	4500215.09	1302.14
VVA-017	430353.38	4507187.21	1411.10
VVA-018	422191.15	4518810.41	1285.94
VVA-019	428289.28	4508582.64	1356.75
VVA-020	427088.82	4497917.29	1346.87
VVA-021	431457.38	4493083.54	1512.15
VVA-022	431116.11	4491238.40	1546.72
VVA-023	431038.58	4487936.10	1554.06
VVA-024	420214.97	4479529.16	1406.21
VVA-025	422881.55	4489610.44	1316.41
VVA-026	428394.13	4484823.97	1398.49
VVA-027	413008.87	4495697.13	1474.65
VVA-028	415945.84	4495786.95	1405.70
VVA-029	421589.92	4506332.53	1292.95
VVA-030	420378.63	4479547.51	1396.86

APPENDIX B – CALIBRATION CONTROL ACCURACY REPORT

Salt Lake Valley LiDAR Aerial Survey			
Survey Point	**Known Z (m)**	**Laser Z (m)**	**Dz (m)**
GCP-101	1287.03	1287.02	-0.01
GCP-102	1286.71	1286.66	-0.05
GCP-103	1502.98	1502.96	-0.02
GCP-104	1415.11	1415.08	-0.03
GCP-105	1425.17	1425.19	0.02
GCP-106	1349.76	1349.74	-0.02
GCP-107	1591.37	1591.32	-0.05
GCP-108	1529.64	1529.66	0.02
GCP-109	1316.49	1316.43	-0.06
GCP-110	1290.82	1290.79	-0.03
GCP-111	1302.35	1302.31	-0.04
GCP-112	1347.66	1347.59	-0.07
GCP-113	1317.98	1317.96	-0.02
GCP-114	1292.89	1292.88	-0.01
GCP-115	1366.60	1366.53	-0.07
GCP-116	1394.78	1394.77	-0.01
GCP-117	1390.42	1390.42	0.00
GCP-118	1496.91	1496.82	-0.09
GCP-119	1322.85	1322.79	-0.06
GCP-120	1442.39	1442.36	-0.03

Average Dz (m)	-0.030
Minimum Dz (m)	-0.090
Maximum Dz (m)	+0.020
Average Magnitude (m)	0.040
RMSE (m)	0.043
Std. Deviation (m)	0.030